International Journal of Innovative Computing, Information and Control
Volume **8**, Number **5(A)**, May **2012**

ICIC International ©2012 ISSN 1349-4198
pp. **2995–3013**

AN AUTOMATIC DRUG IMAGE IDENTIFICATION SYSTEM BASED ON MULTIPLE IMAGE FEATURES AND DYNAMIC WEIGHTS

Rung-Ching Chen[1], Yung-Kuan Chan[2], Ying-Hao Chen[1] and Cho-Tsan Bau[1,3]

[1]Department of Information Management
Chaoyang University of Technology
No. 168, Jifeng E. Rd., Wufeng District, Taichung 41349, Taiwan
crching@cyut.edu.tw

[2]Department of Management Information Systems
National Chung Hsing University
No. 250, Kuokuang Rd., Taichung 402, Taiwan

[3]Taichung Hospital, Department of Health, Executive Yuan
No. 199, San Min Rd., Sec. 1, Taichung 403, Taiwan

Received January 2011; revised August 2011

Abstract. *For patients, correct drug information is important. However, patients always do not possess or comprehend professional drug facts. Many drug recognition systems offer keyword searches based on drug names, which may vary from product to product. A more robust form of search would enable users to describe the features of drugs based on their appearance. In this paper, we propose an automatic drug image identification system (ADIIS) based on multiple image features. ADIIS is able to reduce drug identification errors as well as provide more accurate drug information. In our primary experiments, by using an image, the system is able to retrieve the top ten similar drugs, enabling the user to identify the specific one. Experimental results show that the first drug of the ten identified by ADIIS was the correct drug in 92.6% of tests.*
Keywords: Hamming distance, Gabor filter, Neural network, HSV, CBIR

1. **Introduction.** Accidental medication mishaps occur frequently, making medication safety an important issue [1-5]. Hospitals currently provide a variety of drug counseling in order to rectify these problems. However, many individuals also search for information on their own.

Web searches for medicine information can be performed in two ways: (1) database mapping and (2) keyword search [6]. Database mapping allows users to compare drug images with database information [7]. However, this method is time-consuming and inefficient for drug searches. Keyword search is performed by entering specific words, such as the drug name, color, shape, size, lettering and other features [7-10]. However, since the search is user-defined and provides only limited features for the system, errors in identification are frequent.

Several researchers have proposed drug identification systems using content based image retrieval (CBIR). CBIR is a popular technology of image recognition [11,12] which extracts physical features such as color or shape to describe an image of the object. These features are then used for drug recognition. However, CBIR cannot effectively identify white circular drugs because they cannot produce representative features when drugs have the same shape and color.

In this paper, we will propose an Automated Drug Image Identification System (ADIIS), using content-based image retrieval to extract the features of drug images, and using neural networks, the fuzzy method and relevant feedback, perform drug recognition. The features used to recognize drugs include colors, shapes, ratios, magnitudes and textures. We use these five features in combination with dynamic weight setting for drug identification. The query image is matched with database images of drugs by the weighted Euclidean distance to calculate similarity distance. The system then retrieves ten of the images most similar to the target drug image, allowing the user to correctly identify the drug and obtain information about it. The major contributions and advantages of this paper are to construct an Automated Drug Image Identification System based on five features and dynamic features' weights to identify drugs and improve the recognition accuracy of drugs even they are white circular drugs. Due to that general local clinic provides less than 300 different drugs in Taiwan, we collect the number of drugs' images to test the system. Hence, the system can be applied to clinic's drug recognition for patients and pharmacists.

The remainder of the paper is organized as follows. Section 2 describes relevant drug identification techniques. Section 3 explains the preprocessing and features extraction functions of our proposed system. Section 4 discusses the similarity measurement. Section 5 reports experimental results and discussions. Finally, conclusions and future work are discussed in Section 6.

2. Literature Review.

2.1. Content based image retrieval.

The term content-based image retrieval (CBIR), also known as query by image content, is the application of computer vision techniques to the image retrieval problem of searching for digital images in large databases. The term is also used to describe the procedures necessary to retrieve images from a large collection, based on the syntactic image features. It encompasses technologies, tools and algorithms from areas such as statistics, pattern recognition, signal processing, and computer vision. Though current CBIR systems typically use low-level features such as texture, color and shape, systems that use high-level features such as texture are common. Not every CBIR system is universal. Some systems are designed for a specific area, such as color matching, and can be used to find parts within a medical database. Using CBIR, we exploit different image processing techniques to extract the features of drugs to query a drug database.

2.2. Related of drug identification system.

Many hospitals provide drug information databases for people to identify drugs and their functions. Such drug identification systems may be divided into two types [6]. The first is a list of drug names, where the user selects a similar drug. The second system uses keyword search, including the name (in Taiwan, both English and Chinese), shape, color, pattern and other features. The latter system searches databases to find features of drugs that match the search results [13]. Figure 1 shows a website for a drug identification system [14].

Zeno et al. [15] designed a drug identification system that combines IBM's QBIC (Query by Image Content) and the iMatch system. Zeno extracts features and follows the format of MPEG-7. The features are entered into QBIC and iMatch to identify the specific drug. However, Zeno's proposed method only identifies a small number of drugs, a fraction of the large and constantly expanding number of drugs used.

Hsieh et al. [6] proposed a Real Drug Image Identification System (RDIIS). RDIIS uses the features of color and texture to search for images in a database. However, in the RDIIS, many drugs have similar colors and shapes, meaning that the queried image is often not found.

FIGURE 1. Medication information website using name, form, color and brand

Lin et al. [16] proposed a tablet drug image retrieval system to raise the drug recognition of white tablets. Lin's system extracts features including the shape, color and size. It uses neural networks and combines moment invariants and Zernike moments to identify the drug. However, Lin's method is not effective in identifying drugs, because many drugs are similar, and have the same size and color. This system still cannot effectively extract the representative features of drugs.

Xie et al. [17] captured drug features that users select for system identification, such as drug size, shape, weight and color. Xie's system provides a way for the user to select the features extracted. Because of their popularity, white circular drugs and their features are hard to represent, so the system cannot recognize the specific appearance of the drugs.

Given these problems, we propose a system using five features: color, shape, magnitude, ratio and texture. We incorporate a dynamic weight setting for drug identification [18-22]. Table 1 shows the comparison of the above methods.

TABLE 1. Related drug identification image retrieval research

Authors	Features				
	Shape	Magnitude	Color	Ratio	Texture
Zeno et al. (2001)	V	–	V	–	V
Hsieh et al. (2005)	–	V	V	–	V
Lin et al. (2007)	V	V	V	–	–
Xie et al. (2008)	V	V	V	–	–
Our system (ADIIS)	V	V	V	V	V

3. **Preprocessing and Features Extraction.** In this paper, we propose an Automatic Drug Image Identification System to identify drugs. The ADIIS is shown in Figure 2. It is divided into two phases, the learning phase and the recognition phase. We will describe the functions of each block of the flowchart as follows.

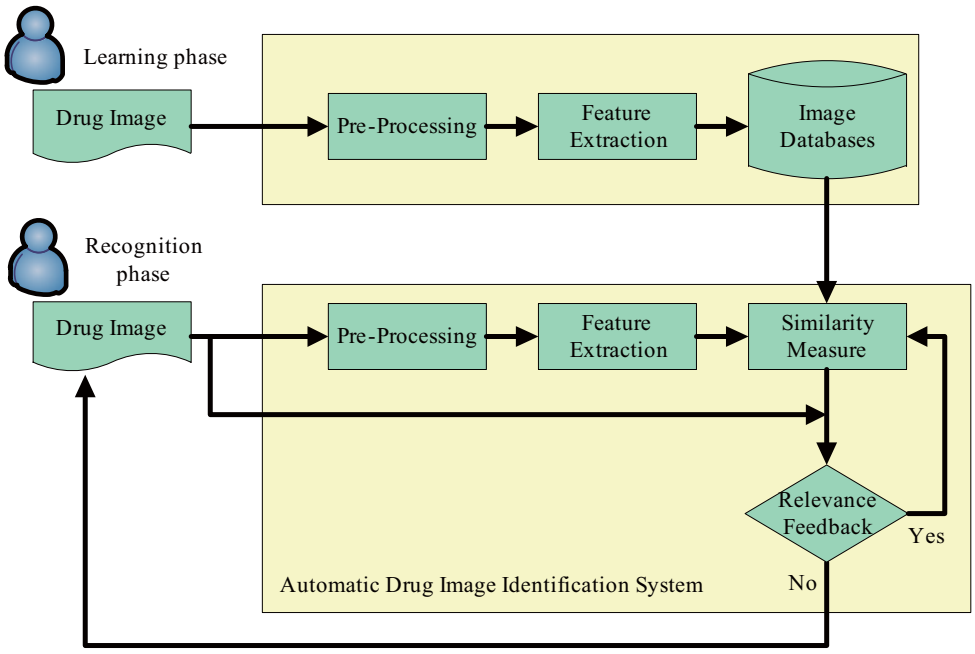

FIGURE 2. Workflow of automatic drug image identification system

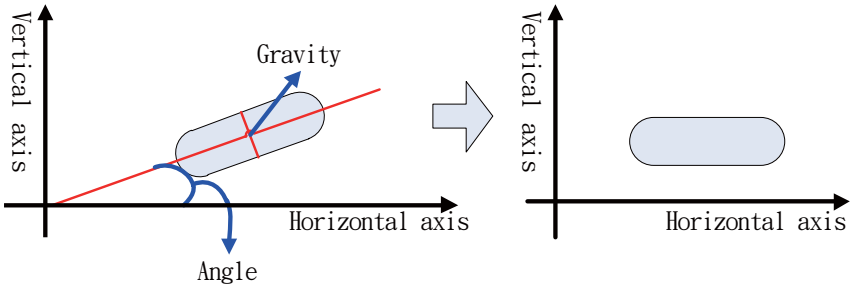

FIGURE 3. Drug rotation angle for preprocessing

3.1. **Pre-processing.** In the pre-processing, the drug images will be normalized to an 800×600 image. Then the system automatically defines the drug, and draws a region of interest (ROI). In the ROI, the drug is white and the background is black. Next, the system will calculate the gravity of the pill [23]. The center of gravity is calculated by rotating the white drug images until they align with the horizontal background graph lines at an angle. We aligned the longer side of the drug to the horizontal axis and the shorter side to the vertical axis. Figure 3 shows the image rotation for pre-processing.

As the drug images may have noise and/or blurred edges, the system uses median filters to eliminate noise and effectively preserve the original texture [24]. In addition, we used histogram equalization to enhance the drug shape and texture. Figure 4 shows the steps of preprocessing.

3.2. **Feature extraction.** The system uses five features to recognize drugs: color, shape, ratio, magnitude and texture. The features extraction and arrangement are specified below.

3.2.1. *Color feature.* In this paper, we used the HSV color space as features for drug identification because it is more stable than the RGB model and the Lab model [25]. The HSV color space is based on hue, saturation and the value of the intensity [26,27]. Drug colors are divided into the following ten colors: white, gray, black, purple, blue,

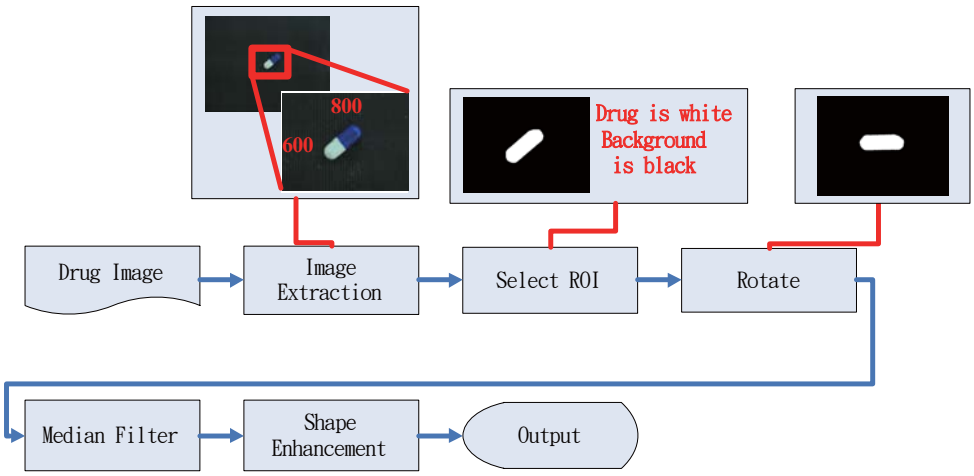

FIGURE 4. Preprocessing instructions related to processes

green, yellow, orange, red and cyan [28]. Table 2 shows the relationship of colors and their corresponding numeric values.

The transformation model is listed below. The images of RGB values were converted into HSV values. The value of hue is obtained through Equation (1). The value of saturation is obtained from Equation (3), and the value of intensity is obtained from Equation (4). C_i is the multiplication of imH_i, imS_i and imV_i shown in Equation (5) where i is the index of the ten colors. If a drug contains two colors on one side, the system calculates the mixed color value C_m using Equation (6).

$$imH = \begin{cases} \theta, & \text{if } imB \leq imG \\ 360 - \theta, & \text{if } imB > imG \end{cases} \tag{1}$$

where imR, imG and imB are the image R, G and B color values and θ is defined as in Equation (2).

$$\theta = \cos^{-1}\left\{ \frac{\frac{1}{2} \times ((imR - imG) + (imR - imB))}{[(imR - imG)^2 + (imR - imB)(imG - imB)]^{\frac{1}{2}}} \right\} \tag{2}$$

$$imS = 1 - \frac{3}{(imR + imG + imB)} \times [\min(imR, imG, imB)] \tag{3}$$

$$imV = \frac{1}{3}(imR + imG + imB) \tag{4}$$

The values of imH, imS and imV are the picture's H, S and V values after R, G and B conversion.

$$C_i = imH_i \times imS_i \times imV_i \tag{5}$$

$$C_m = C_i \times K_1 + C_j \times K_2, \text{ where } C_i > C_j \tag{6}$$

C_i and C_j are different colors in the same drug. K_1 is the weight of C_i, while K_2 is the weight of C_j. In general, K_1 is set to zero and K_2 to 1 when the drug only has one color. If it has two colors, K_1 will be set to 100 and K_2 to 10. In order to limit the image's color feature, we formalize each color feature to a real value between 0 and 1. When the C_m value exceeds 1, the tablet or pill has two colors. We define $C_i > C_j$ that will let two colors drugs have the same values; for example, {(red, blue)} and {(blue, red)} will have the same value of C_m.

TABLE 2. Ten colors mapping value

Color	Black	Green	Red	Blue	Orange	Gray	Yellow	Purple	Cyan	White
imH	0.00	0.50	0.08	0.67	0.25	0.92	0.33	0.83	0.75	1.00
imS	1.00	1.00	1.00	1.00	1.00	1.00	1.00	1.00	1.00	1.00
imV	1.00	1.00	1.00	1.00	1.00	1.00	1.00	1.00	1.00	1.00
C_i	0.00	0.50	0.08	0.67	0.25	0.92	0.33	0.83	0.75	1.00

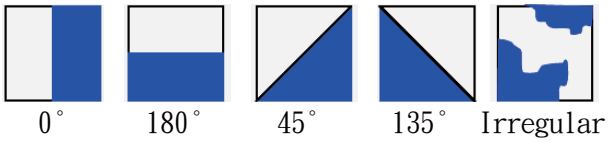

FIGURE 5. Five different types of EHD

Consider a drug composed of both red and blue. The red color value would be multiplied by 0.08 while the blue color value would be multiplied by 0.67 (Table 2). Thus, C_i is 0.67 and C_j is 0.08. The total value, 67.8, would be obtained using Equation (6). In our system, when the color feature value is greater than 1, the drug is composed of compound colors. Hence, using this equation, the system can identify a drug of compound colors. DB_1 is used to represent the value of the color feature.

3.2.2. *Shape feature.* Canny edge algorithm is used to define the edge of the drug images and convert them into binary images [29,30]. The edge is then divided into four equal blocks. An MPEG-7 Edge Histogram Descriptor (EHD) [27] is used for the distribution edge of the drug images [31-33]. Five types of drugs were used to indicate the various shapes of possible edges. Figure 5 shows the five types of EHD.

The values of EHD are sent to a back-propagation neural network to classifier the shape of drug [16]. The neural network has three layers. The input layer has four nodes, the hidden layer has three nodes, and the output layer has 10 nodes. The output layer indicates ten different shapes of drugs: triangular, square, pentagonal, hexagonal, octagonal, rectangular, circular, irregularly-shaped, oval-shaped and long cylindrical [6]. We then map the ten types onto numerical values between 0 and 1. Table 3 shows the mapping results and Figure 6 shows the back-propagation neural network of the shape classification of the feature. DB_2 is used to represent the value of the shape.

TABLE 3. Shape mapping values

Shape	Value
Triangle	0.1
Square	0.2
Pentagon	0.3
Hexagon	0.4
Octagon	0.5
Rectangle	0.6
Circle	0.7
Irregular shape	0.8
Oval	0.9
Long cylindrical	1.0

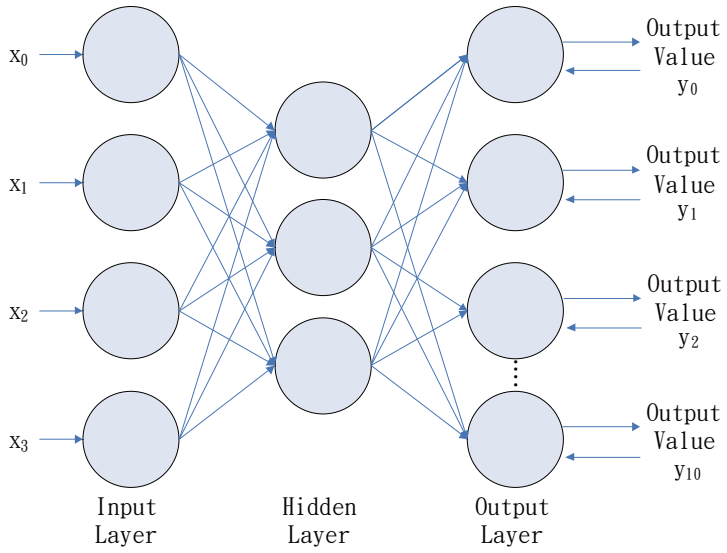

FIGURE 6. Back-propagation neural network for drug shape classification

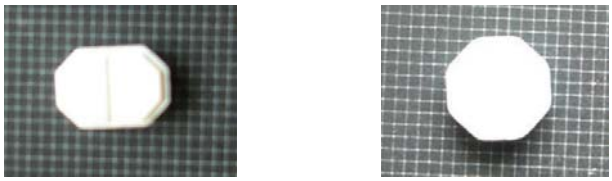

(A) (B)

FIGURE 7. Drugs with similar shapes but different ratios

3.2.3. *Ratio feature.* Ratio is the rate of the maximum width divided by the maximum length, shown in Equation (7).

$$DB_3 = \frac{\max(width)}{\max(length)} \tag{7}$$

Ratio can effectively strengthen the identification of drugs with the same shape but different ratio. Figure 7 shows two drugs that have same shape but different ratios. The ratio feature can be used to distinguish between capsules and tablets, but it is not useful for circular tablets. The value is between 0 and 1.

3.2.4. *Magnitude feature.* We placed the drugs on a black sheet of paper with white grid lines. Magnitude measurement is determined by the area of the grid lines covered by the drug. The system uses the grid lines to measure the magnitude of each drug. Each grid is 1×1 mm square. Due to fact that drugs are rarely black, the black background enhances medication identification. Figure 8 shows the background of the drug images.

We adjust the size of the drug image according to the system settings. First, the drug image is adjusted to the same scale as the system setting. Second, the drug is retrieved. Third, the pixels of the drug are calculated. After detecting the size of the drug, we then retrieve drugs from small to large in the database. The system selects the drugs with a magnitude closely matching that of the measured drug. The Hamming distance is then used to calculate the difference, as shown in Equation (8).

$$DB_4 = \left(\frac{\min\{Q, D_n\}}{\max\{Q, D_n\}} \right) \tag{8}$$

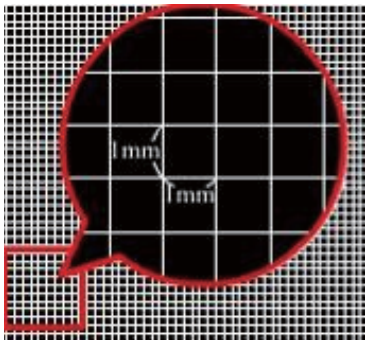

FIGURE 8. Background of drug images (1 × 1 mm grid)

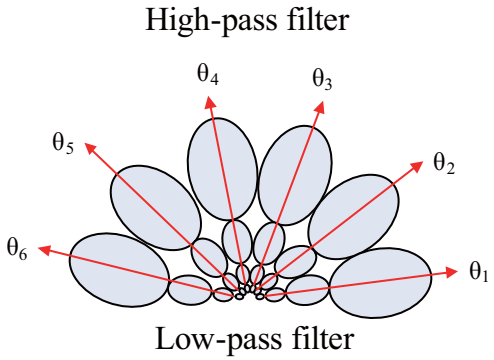

FIGURE 9. A Gabor filter

In Equation (8), Q is the magnitude of the query drug, and n is an index. D_n is the magnitude of drug images with index n in the database. Thus, the value of DB_4 is between 0 and 1. When the value of DB_4 is equal to 1, it means that the two drugs have exactly the same magnitude.

3.2.5. *Texture feature.* The Gabor filter is used to calculate the drug texture [33-38]. First, the surface texture of the drug is converted into a binary image. Second, the Canny edge algorithm is used to calculate the value of the edge pixels [39]. Third, the texture of the drug edge is removed. Equation (9) shows the expression of the Gabor filter:

$$g_\sigma(x,y) = \left(\frac{1}{2\pi\sigma_x\sigma_y}\right) \exp\left(\frac{-1}{2}\left(\frac{x^2}{\sigma_x^2} + \frac{y^2}{\sigma_y^2}\right)\right) \tag{9}$$

In this equation, x, y is the input image, and σ is bandwidth of Gaussian filter [37]. Last, $g_\sigma(x,y)$ is processed in a two-dimensional Gabor filter in Equation (10).

$$G(x,y) = g_\sigma(x,y)\exp(2\pi jW(x\cos\theta + y\sin\theta)) \tag{10}$$

In this equation, W is the frequency of the input texture image and θ is the image frequency of the projection direction. The output value is between 0 and 1. Figure 9 shows a Gabor filter [31]. DB_5 is used to represent the feature.

4. **Similarity Measurement and Relevance Feedback.**

4.1. **Similarity measurement.** When the system completes the features extraction of test drugs features, the vector of features is defined as follows:

$$feature(Q_i) = (q_1, q_2, q_3, q_4, q_5) \tag{11}$$

q_1 is the color feature of test drugs, q_2 is the shape feature, q_3 is the ratio feature, q_4 is the magnitude feature and q_5 is the texture feature.

In addition, the features of drugs in the database are represented as follows:

$$feature(DB_i^n) = (DB_1^n, DB_2^n, DB_3^n, DB_4^n, DB_5^n) \tag{12}$$

n is the index of images in database. DB_1^n is the color feature, DB_2^n is the shape feature, DB_3^n is the ratio feature, DB_4^n is the magnitude feature and DB_5^n is the texture feature.

The white circular tablet drugs appear to be difficult to recognize due to the fact that many are similar in size, color and shape. Determining the surface texture of the drugs is useful in correctly verifying these drugs. To be able to effectively identify these drugs, the weight of Euclidean distance is used as shown in Equation (13). Our experiments indicate that the square of m is 1.6 can obtain better results. We use the dynamic weights of the features to improve the accuracy of the system identification:

$$Sim_n^q = \left(\sum_{i=1}^{5} W_i \times (X_i)^m \right)^{\frac{1}{2}} \tag{13}$$

$$X_i = q_i - DB_i^n$$

where

$$w_1 + w_2 + w_3 + w_4 + w_5 = 1$$

$$X_1 = \begin{cases} X_1 = 0 & \text{when } q_1 == DB_1^n \quad // \text{ the same color} \\ X_1 = 1 & \text{when } q_1 \neq DB_1^n \quad // \text{ different color} \end{cases}$$

$$X_2 = \begin{cases} X_2 = 0 & \text{when } q_2 == DB_2^n \quad // \text{ the same color} \\ X_2 = 1 & \text{when } q_2 \neq DB_2^n \quad // \text{ different color} \end{cases}$$

w_1 is the weight of the color feature, w_2 is the weight of the shape feature, w_3 is the weight of the ratio feature, w_4 is the weight of the magnitude feature and w_5 is the weight of the texture feature.

To obtain the drug image in the database which matches the features of the queried drug images, the system uses the weighted Euclidean distance to measure the similarity between the test image and the candidate image. Weights are set based on fuzzy rules. This decision proves the definition of the internal parameters. For example, color, shape and ratio features are valueless for white circular drugs, so they are set to 0.

Rule 1: IF color is white and shape is circular;
THEN w_5 is K, w_4 is $1 - K$, and $w_1 = w_2 = w_3 = 0$;
where $K = \frac{M-0.1}{0.8}$

K is decided by the magnitude and texture. M is the magnitude value. If the size is larger, the weight of the texture is smaller. Figure 10 is shows the adjustment of relations of the weight between the magnitude and texture and the linear equation $K = \frac{M-0.1}{0.8}$.

In addition, when the shape of the test drug is oval, and has two colors, the system classifies it as a capsule and increases its weight based upon its color features.

Rule 2: IF shape is oval-type and $C_p > 1$;
THEN w_1 is K_1, w_4 is $1 - K_1$, and $w_2 = w_3 = w_5 = 0$;
where $K_1 = K_{cp} \times (C_p - 0.8)$

K_1 is the weight value. $K_{cp} = 0.098$. When the weight of the color is larger, the weight of the magnitude is smaller. Figure 11 shows the adjustment of the relations between color and magnitude. Determining the texture of the capsule drugs is difficult, so the system did not consider texture when determining classification.

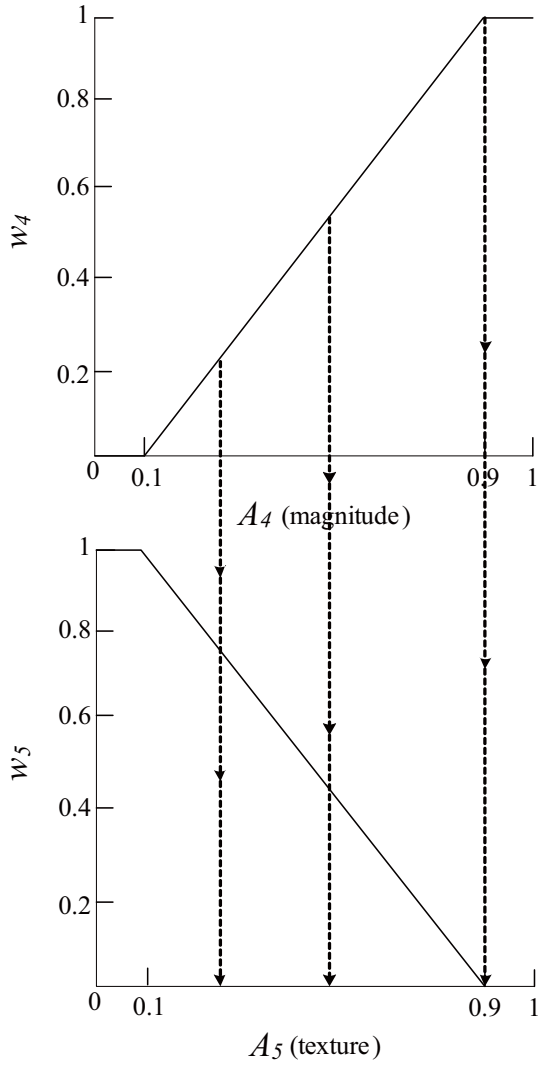

FIGURE 10. Relationship between white circular drug weights

The Euclidean distance value is smaller when the test drug image is similar to the drug in the database. According to the results of the calculation, the system selects the most similar drug images and outputs the top ten most similar drug images to the users. The output information includes drug images and drug names. The similarity measurement workflow of the system is shown in Figure 12. First, the feature values of the drug's image are entered into the system. Next, the system processes shape and color recognition. If the color is white and circular, Rule 1 is used to set the magnitude and texture weights, by following the dynamic value to adjust the weight of K. If the drug's color is compound and its shape is oval, Rule 2 is used to set the weights of color and magnitude. When the shape is neither circular nor oval, then the weights are equal and set to 0.2. The next step is to select the candidate of magnitude, and calculate the similarity of the drug image to the images in the database. The drug feature's values and weights are then uploaded to the system, which calculates the similarity measurement. Finally, the system outputs the rankings of matching drugs to the user.

4.2. **Relevance feedback.** In CBIR and other image retrieval systems, one difficulty is how to use the low-level image features to describe the high-level visual images that users

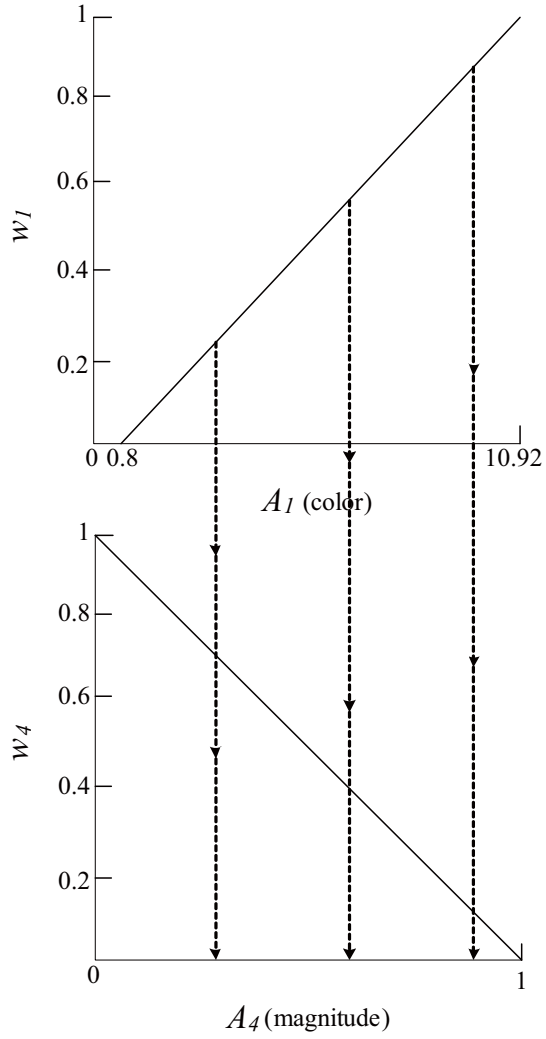

FIGURE 11. Fuzzy membership for oval drug weight

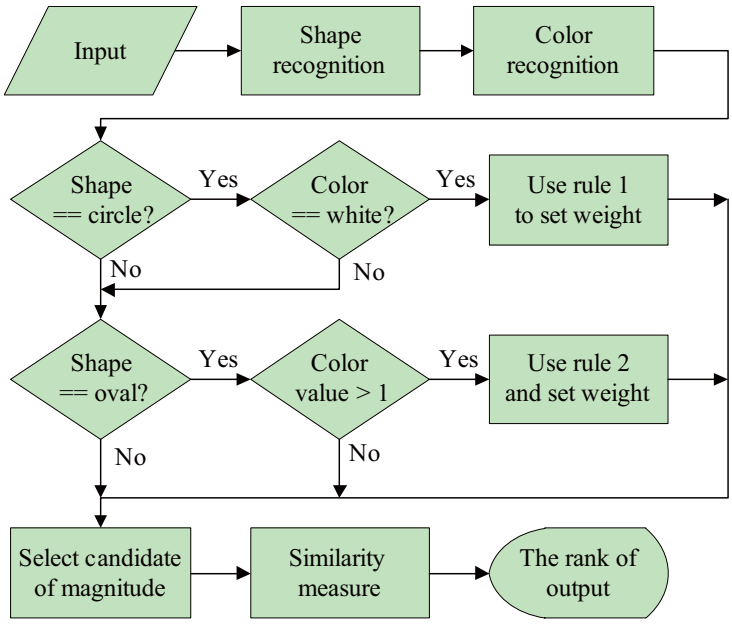

FIGURE 12. Workflow of similarity measurement

define [39-42]. In other cases, the programs use an algorithm or similarity measurement to measure the similarity of retrieved images to query images. Generally, only one or two algorithms are used to estimate similarity in their system. Hence, if the system only uses a similarity measurement to determine that two images are related, it is difficult to meet the needs of different users. Therefore, some systems offer an interactive approach for retrieved images. This interaction, termed relevance feedback, means that the system adds the users subject to the image identification. The relevance feedback is divided into two types, positive and negative. A positive image is related to query image, while a negative image is unrelated. First one is positive relevant. It selects some positive images about user's query image from query results. The second is negative relevance. It selects some negative images about user's query image from query results. When the system checks the database again it will use the positive/negative feedback.

In general, there are two approaches to the use of relevant feedback. One approach uses feedback to adjust several parameters of the similarity measurement [6,41], such as weights. The other approach uses the concept of probability [6]. It obtains the probability of every image in database, return high probability images to the user.

In this paper, we used the similarity measurement to identify drugs and to adjust the feature weights. If we use the first approach, it may be overstep the region of weight value when the system identifies white circular drugs and capsules. Thus, we use the second method to compensate for the semantic gap. Conditional probability was used to find candidate drugs, seen in Equation (14).

$$Pb(A_i) = \sum_n Pb(A_i|B_n)Pb(B_n) \tag{14}$$

A_i is ith candidate drug image. $Pb(A_i)$ is the probability of ith candidates. B_n was the positive candidates. The steps of the relevance feedback are listed as follows:

(1) The system will confirm the positive and negative relevant feedback that users provide.
(2) The system matches the features of the feedback and the candidate drugs and then gives the weight values of the relevance to the candidates images. Weights close to 1 mean that candidate drugs are positive and close, while weights close to zero show images that are negative and unrelated.
(3) Finally, the system outputs the high probability candidate drugs to users, and deletes the low probability candidates.

Figure 13 shows the workflow of the relevance feedback. First, the system records the feedback information about positive and negative drug images. Second, if users set the value to 'null', the system will not calculate the probability values of $Pb(A_i)$. Third, the feedback information helps map features of candidates whose selection is then based on our similarity measure. We map each candidate and confirm whether it is positive or negative. Fourth, if the candidate is positive, we use the positive images to query the system. These results are ranked based on the similarity values. If the candidate is negative, we delete this candidate from the output results. Finally, we output the top ten positive images for the user. If the results do not meet the needs of the user, our system gives users the ability to provide feedback again. If users select the 'Null' button for all results the system is finished with its identification.

5. **Experiments and Discussions.**

The system was implemented in Matlab7.0. Table 4 lists the hardware of the experimental environment. The drugs were provided by Taichung hospital in Taiwan. 263 drugs were used in this paper, including medicines for diabetes, blood pressure, colds and antibiotics. Of these, 82 were white circular drugs, while 48 were capsule drugs. Two images were taken of each drug to document both sides, resulting in

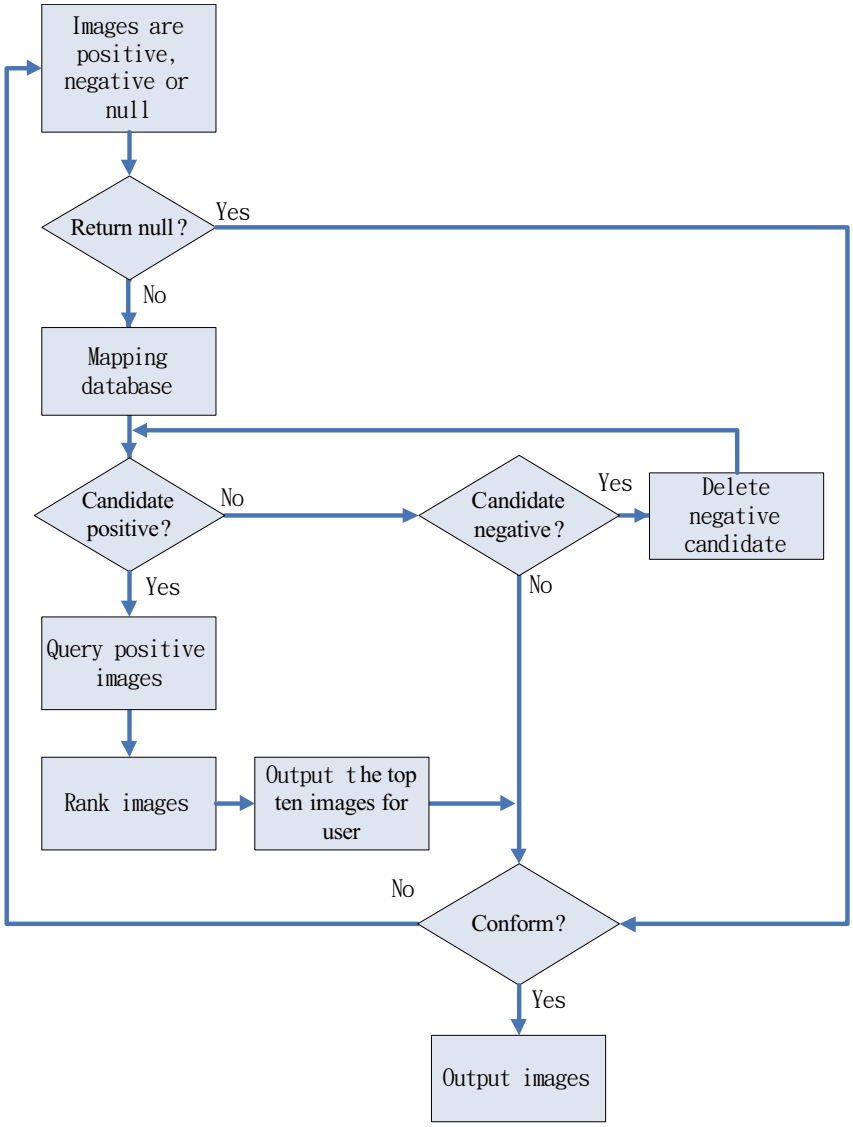

FIGURE 13. Workflow of relevance feedback in the ADIIS system

526 drug images. The accuracy rate of the system is calculated according to the following formula:

$$Accuracy = \frac{\text{The Number of Correct Classification Images}}{\text{Total Number of Query Images}} \tag{15}$$

TABLE 4. Computer hardware used in the experiment

Hardware	Specifications
CPU	AMD 1.6 GHz
Video Controller	256 MB
Memory	1 GB
Hard disk	80 GB

In the similarity measure, the drugs are divided into general drugs, white circular drugs and capsules. The weights of features are based on these classifications. We use cross-validation to validate the classification accuracy of the system. First, we divide the drugs

into groups A and B. Group A is the training data, used to provide the system with information for drug classification. Group B is the test data. In this step, the average recognition accuracy is 97% for general drugs, for white circular drugs, 100%, and for capsules, 96%. Second, we use group B as the training data and group A as the test data. In this step, the average recognition accuracy rate is 98% for general drugs, for white circular drugs it is 100%, and for capsules it is 97%.

Our system for the classification of the three types of drugs offers good results. The reason why general drugs have lower accuracy than cylindrical drugs is the capsule. Capsules have 97% accuracy since some capsules are the same color at both ends.

In addition, we design five experiments to test the accuracy of our system and check the accuracy after we add relevance feedback how the accuracy is enhanced. Due to that most of drugs recognition systems only test for randomly selecting drugs test, hence we compare our method with Hsieh's method which the better method has been published until now. The five types of experiments are randomly selecting drugs test, the white circular drugs, non-white circular drugs, all circular drugs and capsules. The detail experiments are shown as the following.

5.1. **Experimental 1: randomly selecting drugs.** This test was performed ten times. Thirty drug images were selected randomly each time. For example, in Test 1, we used thirty drug images as test images. Twenty eight drugs were recognized in rank1, the remaining two were determined to be rank2 and rank3. Table 5 shows the average accuracy results and Figure 14 shows the results of four test runs. We can see that by rank6 all drugs had been successfully identified by the system. The average recognition accuracy rate is 92.6% for rank1.

In Table 5, the accuracy value of Test 8 is lower than the other tests, because it has three similar white circular drugs and one capsule was a similar color to the database in rank1. In rank2, the system remains unable to identify the four drugs. In rank3, the system identified two drugs, but in it two drugs were not successfully identified. By rank6 all drugs had been successfully identified. The identification results of our system are better than those of the proposed systems of Lin [16] and Hsieh [6].

In this experiment, our system is able to identify drugs with an accuracy rate of 92.6% in rank1, while Hsieh's [6] proposed system only identified 82.82%. Hsieh's proposed system cannot effectively identify white circular drugs, lowering its recognition rate. Our system adjusts the differing weights based on the drugs, to enable it to process a wide variety of drugs.

TABLE 5. Accuracy of ten test runs

Rank	Test 1	Test 2	Test 3	Test 4	Test 5	Test 6	Test 7	Test 8	Test 9	Test 10	Average
Rank1	93	90	93	97	90	93	93	87	93	97	92.6
Rank2	97	93	97	100	97	93	97	87	97	100	95.8
Rank3	100	93	97	100	100	97	97	93	97	100	97.4
Rank4	100	100	100	100	100	100	100	97	100	100	99.7
Rank5	100	100	100	100	100	100	100	97	100	100	99.7
Rank6	100	100	100	100	100	100	100	100	100	100	100

We used the feedback to adjust our system. Table 6 shows the results of the relevance feedback in this experimental. It shows that the recognition rate is enhanced by relevance feedback. In Test 8, there are three similar white circular drugs, and their texture features are not significant. However, our system can reduce identification in the rank and the results are shown among the top four outcomes.

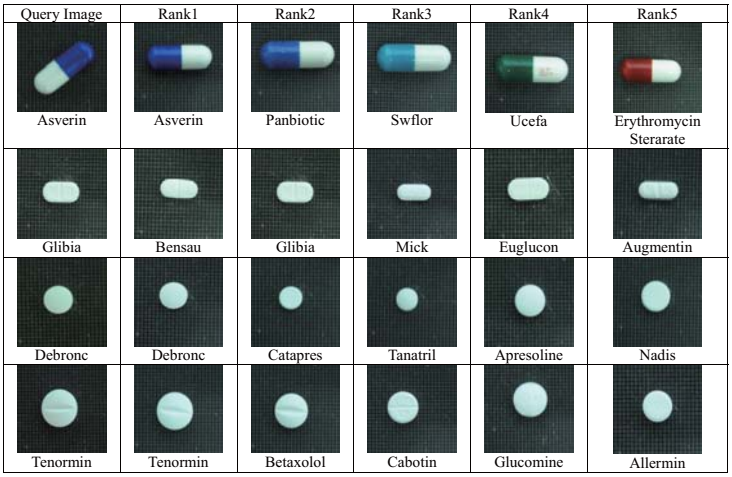

FIGURE 14. Randomly selected results of three test runs

TABLE 6. Relevance feedback by randomly selecting result

Rank	Test 1	Test 2	Test 3	Test 4	Test 5	Test 6	Test 7	Test 8	Test 9	Test 10	Average
Rank1	97	97	93	100	93	93	93	93	97	97	95.3
Rank2	100	100	97	100	97	100	97	97	100	100	98.8
Rank3	100	100	100	100	100	100	97	100	100	100	99.7
Rank4	100	100	100	100	100	100	100	100	100	100	100

5.2. **Experimental 2: the drug is white and circular.** Since the system has difficulties recognizing white circular drugs, we designed another experiment to identify only white circular drugs. In this experiment, we selected 82 white circular drugs from among the 263 test drugs. The test was run ten times. Twenty drug images were randomly selected from the 82 candidate drugs. This experiment confirms that our system can effectively identify white circular drugs. Table 7 shows the experimental results of the ten tests done on white circular drugs. Each test was performed by identifying 20 white circular drugs images, and was completed with an average accuracy rate of 80.5% in rank1. Our system is able to identify 80.5% of white circular drugs in rank1, while Hsieh's proposed system only identified 74%. Therefore, our system's identification of white circular drugs is better than Hsieh's.

TABLE 7. The accuracy of ten times test of white circular drug results

Rank	Test 1	Test 2	Test 3	Test 4	Test 5	Test 6	Test 7	Test 8	Test 9	Test 10	Average
Rank1	80	75	85	80	75	85	90	70	80	85	80.5
Rank2	90	85	90	90	85	85	90	80	85	90	87
Rank3	95	90	100	95	90	95	95	95	85	90	93
Rank4	100	90	100	100	95	100	100	100	90	95	97
Rank5	100	100	100	100	100	100	100	100	90	100	99
Rank6	100	100	100	100	100	100	100	100	90	100	99
Rank7	100	100	100	100	100	100	100	100	95	100	99.5
Rank8	100	100	100	100	100	100	100	100	95	100	99.5
Rank9	100	100	100	100	100	100	100	100	100	100	100

In this experiment, the test images included drugs with the same magnitude and non-texture drugs. The accuracy value of Test 7 is lower than the other tests because it

TABLE 8. Relevance feedback: white circular drug results

Rank	Test 1	Test 2	Test 3	Test 4	Test 5	Test 6	Test 7	Test 8	Test 9	Test 10	Average
Rank1	90	85	90	85	80	90	90	85	80	95	87
Rank2	100	95	95	95	90	90	95	95	85	100	94
Rank3	100	100	100	100	95	100	100	95	90	100	98
Rank4	100	100	100	100	100	100	100	100	90	100	99
Rank5	100	100	100	100	100	100	100	100	95	100	99.5
Rank6	100	100	100	100	100	100	100	100	100	100	100

contained many drugs with the same magnitude as well as non-texture drugs. However, our system was able to identify drugs with an accuracy rate of 100% in rank9. This system demonstrates that size and texture are important features when drugs have the same color and shape features. In the experiment, we found that if the drugs have the same shape and color, and the surface has no texture, the system still found it difficult to identify the drugs.

We used the feedback to adjust the white circular drug identification. Table 8 shows the results of the relevance feedback in this experimental. Our system improves the ranking of the correct results: all are shown in the top 6 outcomes. Test 9 contains four similar white circular drugs, and their texture features are not significant.

5.3. **Experimental 3: the drug is not white but shape is circular.** We also tested non-white circular drugs and all circular drugs. In this experiment, there were 74 non-white circular drugs. The test was performed five times. Twenty drug images were randomly selected. Table 9 shows the results of non-white circular drugs. The results show that our system is able to effectively identify non-white circular drugs.

We used the relevance feedback to adjust the non-white circular drug identification results. Table 10 shows the results of the relevance feedback in non-white circular drugs identification. Our system used the relevance feedback to help drug identification reach nearly 100%, with the correct drug almost always displayed in the first or second outcome.

TABLE 9. Accuracy of the non-white circular drug test

Rank	Test 1	Test 2	Test 3	Test 4	Test 5	Average
Rank1	95	90	100	100	100	97
Rank2	100	95	100	100	100	99
Rank3	100	100	100	100	100	100

TABLE 10. Relevance feedback for non-white circular drug test

Rank	Test 1	Test 2	Test 3	Test 4	Test 5	Average
Rank1	100	95	100	100	100	99
Rank2	100	100	100	100	100	100

5.4. **Experimental 4: all circular drugs.** This test includes all circular drugs that our system is able to effectively identify. Twenty drug images were selected randomly from among 156 drugs. Table 11 shows the results of ten tests of circular drugs.

In Test 9, the system identifies all of the drugs within rank7. Because Test 8 contains a white circular drug and a non-texture drug, its accuracy value is lower than the other tests

in rank1, for some white circular drugs in this test. Thus, it can identify the drug correctly in rank1. We used the relevance feedback to adjust the circular drug identification results. Table 12 shows the results of the relevance feedback in circular drug identification.

In this experiment, without relevance feedback our system accuracy is 85.5%. When we use relevance feedback, accuracy rises to 93.5%. White circular drugs affect the identification of circular drugs, but the system remains able to identify the drug within rank5.

TABLE 11. Circular drug test accuracy

Rank	Test 1	Test 2	Test 3	Test 4	Test 5	Test 6	Test 7	Test 8	Test 9	Test 10	Average
Rank1	90	85	85	85	85	90	90	75	85	85	85.5
Rank2	90	90	90	85	90	90	95	90	85	90	89.5
Rank3	95	90	100	90	95	95	95	95	90	90	93.5
Rank4	100	90	100	90	95	100	100	100	95	100	97
Rank5	100	100	100	100	100	100	100	100	95	100	99.5
Rank6	100	100	100	100	100	100	100	100	95	100	99.5
Rank7	100	100	100	100	100	100	100	100	100	100	100

TABLE 12. Relevance feedback in circular drug results

Rank	Test 1	Test 2	Test 3	Test 4	Test 5	Test 6	Test 7	Test 8	Test 9	Test 10	Average
Rank1	95	95	95	95	90	95	100	85	90	95	93.5
Rank2	100	95	100	95	95	100	100	95	90	95	96.5
Rank3	100	100	100	100	95	100	100	100	95	100	99
Rank4	100	100	100	100	100	100	100	100	95	100	99.5
Rank5	100	100	100	100	100	100	100	100	100	100	100

5.5. **Experimental 5: the capsules.** In this experiment, we select 48 capsules from among the 263 drugs for the test. This test was performed five times, and twenty drug images were randomly selected. Table 13 shows the results of the capsule test. The average recognition accuracy rate is 93% for rank1. The system identifies capsules within the top 4 of all retrieved drug identifications. We use the relevance feedback to adjust the capsule identification results. Table 14 shows the results of the relevance feedback in capsule identification. Our system used relevance feedback to help drug identification attain nearly 100% recognition, with all correct results falling in either rank1 or rank2.

TABLE 13. Capsule test results

Rank	Test 1	Test 2	Test 3	Test 4	Test 5	Average
Rank1	95	90	90	95	95	93
Rank2	95	95	95	100	100	97
Rank3	100	100	95	100	100	99
Rank4	100	100	100	100	100	100

6. **Conclusions and Future Work.** In this paper, we have proposed an automated drug image identification system using multiple image features that adjusts the features weights to identify drugs. In our system, users input a drug image onto the black background. Our system will then automatically identify the drugs users provide. The average recognition accuracy rate is 95.3% in rank1 of random selection tests using relevance feedback to

TABLE 14. Relevance feedback: capsule results

Rank	Test 1	Test 2	Test 3	Test 4	Test 5	Average
Rank1	95	100	95	100	100	98
Rank2	100	100	100	100	100	100

adjust the answers. The experiment confirms that our method for drug identification is feasible and effective, especially for white circular drugs. However, the system still errs with drugs of similar color, magnitude and texture.

In future work, we will explore the use of other digital devices such as mobile phones to access and operate the system. We also recommend including more robust drug information, such as drug ingredients and side effects, to enhance the value of the drug identification system.

Acknowledgement. The authors would like to thank the research support from National Science Council, Taiwan, with number: NSC 98-2221-E-324-031.

REFERENCES

[1] M. A. Moreno and F. Furtner, Medication safety for children, *Archives of Pediatrics and Adolescent Medicine*, vol.164, no.2, pp.208, 2010.

[2] S. Arivazhagan, L. Ganesan and S. P. Priyal, Texture classification using Gabor wavelets based rotation invariant features, *Pattern Recognition Letters*, vol.27, no.16, pp.1976-1982, 2006.

[3] W. Chen, P. J. Chao and H. L. Lin, Drug identification by network adaptive content-based image retrieval, *The Journal of Health Science*, vol.9, no.2, pp.133-145, 2007.

[4] J. X. Du, D. S. Huang, X. F. Wang and X. Gu, Shape recognition based on neural networks trained by differential evolution algorithm, *Neurocomputing*, vol.70, no.4-6, pp.896-903, 2007.

[5] D. Grandt, Improving medication safety, *U.S. National Library of Medicine National Institutes of Health*, vol.52, no.12, pp.1161-1165, 2009.

[6] C. H. Hsieh, *Applying Content Based Image Retrieval to Drug Identification Research*, Master Thesis, Graduate Institute of Medical Information, Taipei Medical University, Taiwan, 2005.

[7] *Medication Information of Taichung Armed Force General Hospital*, http://web-reg-server.803.org.tw:8090/Med_Web/index.asp, 2010.

[8] *Medication Information of Changhua Christen Hospital*, http://www.cch.org.tw/DRUG_01.aspx, 2010.

[9] *Medication Information of Chang Gung Medical Foundtion*, http://www.cgmh.org.tw/stor/drug001.asp, 2010.

[10] *Medication Information of Department of Health, Executive Yuan*, http://drug.doh.gov.tw, Taiwan, 2010.

[11] C. H. Lin, R. T. Chen and Y. K. Chan, A smart content-based image retrieval system based on color and texture feature, *Image and Vision Computing*, vol.27, no.6, pp.658-665, 2009.

[12] Y.-K. Chan, P.-Y. Pai, R.-C. Chen and C.-C. Chang, A VQ compression method based on the variations of the image block groups, *International Journal of Innovative Computing, Information and Control*, vol.6, no.10, pp.4527-4537, 2010.

[13] T. Y. L. Sung, F. H Hung and H. W. Chiu, Implementation of an integrated drug information system for inpatients to reduce medication errors in administrating stage, *Proc. of the 30th Annual International Conference of the IEEE Engineering in Medicine and Biology Society*, pp.743-746, 2008.

[14] *http://www.rxlist.com/pill-identification-tool/article.htm.*

[15] Z. Geradts, H. Hardy, A. Poorman and J. Bijhold, Evaluation of contents based image retrieval methods for a database of logos on drug tablets, *Image Analysis and Characterization of SPIE*, vol.4232, pp.553-562, 2001.

[16] C. H. Lin, E. W. Huang and W. W. Jiang, Pill image retrieval using neural networks, *The Journal of Taiwan Association for Medical Informatics*, vol.16, no.7, pp.29-42, 2007.

[17] Y. Z. Xie, *Study of Drug Identification System Using the Image Processing Technique*, Master Thesis, Department of Electronic Engineering, I-Shou University, Taiwan, 2008.

[18] H. Cao, L. Yi, Z. Pei and G. Liu, A method to determine the weights of features for classification, *ICIC Express Letters*, vol.5, no.5, pp.1667-1672, 2011.
[19] X. Jiang, T. Sun, B. Chen, R. Li and B. Feng, A novel video content understanding scheme based on feature combination strategy, *Journal of Computers*, vol.4, no.7, pp.615-622, 2009.
[20] G. H. Liu, L. Zhang, Y. K. Hou, Z. Y. Li and J. Y. Yang, Image retrieval based on multi-text on histogram, *Pattern Recognition*, vol.43, no.7, pp.2380-2389, 2010.
[21] Z. Liu and C. Liu, Fusion of color, local spatial and global frequency information for face recognition, *Pattern Recognition*, vol.43, no.8, pp.2882-2890, 2010.
[22] M. Pavlou and N. M. Allinson, Automated encoding of footwear patterns for fast indexing, *Image and Vision Computing*, vol.27, no.4, pp.402-409, 2009.
[23] Y. R. Huang, *The Study of Uterine Cervical Cellular Images Based on PC-Based Cytopathologic Image Analysis System and Support Vector Machine*, Master Thesis, Department of Information Management, Chaoyang University of Technology, Taiwan, 2007.
[24] G. Woods, *Digital Image Processing*, Gonzalez, Rafael Inc, 2002.
[25] R. Min and H. D. Cheng, Effective image retrieval using dominant color descriptor and fuzzy support vector machine, *Pattern Recognition*, vol.42, no.1, pp.147-157, 2009.
[26] T. Gevers and A. W. M. Smeulders, Color-based object recognition, *The Journal of the Pattern Recognition Society*, vol.32, pp.453-464, 1999.
[27] Wikipedia, *http://en.wikipedia.org/wiki/Portal: Contents*, 2010.
[28] H. Jegou, M. Douze and C. Schmid, Improving bag-of-features for large scale image search, *International Journal of Computer Vision*, vol.87, no.3, pp.316-336, 2010.
[29] X. Gao, B. Xiao, D. Tao and X. Li, Image categorization: Graph edit distance + edge direction histogram, *Pattern Recognition*, vol.41, no.10, pp.3179-3191, 2008.
[30] E. Tapia, P. Bulacio and L. Angelone, Recursive ECOC classification, *Pattern Recognition Letters*, vol.31, no.3, pp.210-215, 2010.
[31] A. Abdullah, R. C. Veltkamp and M. A. Wiering, Fixed partitioning and salient points with MPEG-7 cluster correlograms for image categorization, *Pattern Recognition*, vol.43, no.3, pp.650-662, 2010.
[32] T. Wu and Y. Gao, Image data field model for edge detection, *ICIC Express Letters*, vol.5, no.3, pp.733-739, 2011.
[33] *MPEG-7 Overview*, http://mpeg.chiariglione.org/standards/mpeg-7/mpeg-7.htm#E11E4, 2010.
[34] M. Arif, Evaluation of discrimination power of features in the pattern classification problem using Arif index and its application to physiological datasets, *International Journal of Innovative Computing, Information and Control*, vol.7, no.2, pp.525-536, 2011.
[35] R. Sandler and M. Lindenbaum, Optimizing Gabor filter design for texture edge detection and classification, *International Journal of Computer Vision*, vol.84, no.3, pp.308-324, 2009.
[36] L. L. Shen and Z. Ji, Gabor wavelet selection and SVM classification for object recognition, *Acta Automatica Sinica*, vol.35, no.4, pp.350-355, 2009.
[37] Y. Zheng, Breast cancer detection with Gabor features from digital mammograms, *Algorithms*, vol.31, no.1, pp.44-62, 2009.
[38] J.-B. Li, H. Gao and J.-S. Pan, Common vector analysis of Gabor features with kernel space isomorphic mapping for face recognition, *International Journal of Innovative Computing Information and Control*, vol.6, no.9, pp.4055-4064, 2010.
[39] R. Phan and D. Androutsos, Content-based retrieval of logo and trademarks in unconstrained color image databases using color edge gradient co-occurrence histograms, *Computer Vision and Image Understanding*, vol.114, no.1, pp.66-84, 2009.
[40] Y. Liu, D. Zhang, G. Lu and W. Y. Ma, A survey of content-based image retrieval with high-level semantics, *Pattern Recognition*, vol.40, no.1, pp.262-282, 2007.
[41] J. A. Santos, C. D. Ferreira, R. S. Torres, M. A. Goncalves and R. A. C. Lamparelli, A relevance feedback method based on genetic programming for classification of remote sensing images, *Information Sciences*, pp.1-14, 2010.
[42] H. V. Sijs, T. V. Gelder, A. Vulto, M. Berg and J. Aarts, Understanding handling of drug safety alerts: A simulation study, *International Journal of Medical Informatics*, vol.79, no.5, pp.361-369, 2009.